A STUDY OF THE EFFECT OF CYCLING MODES ON THE ELECTROCHROMIC PROPERTIES OF Ni(OH)₂ FILMS

V. Kotok
PhD, Associate Professor
Department of Processes, Apparatus
and General Chemical Technology*
E-mail: valeriykotok@gmail.com
PhD, Senior Researcher
Competence center
"Ecological technologies and systems"**
V. Kovalenko
PhD, Associate Professor
Department of Analytical Chemistry
and Chemical
Technologies of Food Additives and Cosmetics*
E-mail: vadimchem@gmail.com
PhD, Senior Researcher
Competence center
"Ecological technologies and systems"**
*Ukrainian State University of
Chemical Technology
Gagarina ave, 8, Dnipro, Ukraine, 49005
** Vyatka State University
Moskovskaya str., 36, Kirov,
Russian Federation, 610000

В результаті проведених досліджень була отримана серія електрохромних плівок на основі Ni(OH)₂ осаджених катодним темплатним методом в однакових умовах. Отримані плівки були використані для порівняння режимів, в яких здійснюється процес затемнення-освітлення. При цьому також були оцінені основні якісні характеристики – середня абсолютна ступінь затемнення, середня незворотність при освітленні і проведено візуальне порівняння плівок в затемненому стані після циклування.

Для визначення впливу різних режимів були запропоновані потенціодинамічні, гальваностатичні і складні режими. Для потенціодинамічних режимів були обрані різні верхні і нижні межі потенціалів-границь циклування. В якості вихідної густини струму для гальваностатичних та складних режимів була обрана густина струму отримана з циклічної вольт амперної кривої. Обрана густина струму відповідала щільності струму катодного піку на п'ятому циклі циклічної вольтамперної кривої знятої в наступному режимі: інтервали потенціалу електрода [201–751 мВ], швидкість розгортки 1 мВ/с.

Проведення процесу затемнення-освітлення в різних режимах показало високу ефективність потенціодинамічних режимів, які дають найбільший ступінь затемнення електрохромного покриття. З іншого боку було показано, що звуження і розширення граничних потенціалів циклування за межі оптимальних, веде до значного погіршення електрохромних характеристик плівок. Гальваностатичні режими показали найбільш оптимальні результати з точки зору абсолютної глибини затемнення і часу затемнення та освітлення. Складні режими показали найгірші результати серед всіх запропонованих. У результаті використання цих режимів абсолютна незворотність при освітленні була значна, а швидкість затемнення та освітлення середня.

У гальваностатичних та складних режимах було знайдено дві струмові площадки на кривих густина струму-час, що може говорити при наявність двох фаз у електрохромному матеріалі: α-Ni(OH)₂ та β-Ni(OH)₂

Ключові слова: електрохромізм, циклування, циклічна вольтамперометрія, гальваностатичний, потенціостатичний електроосадження, Ni(OH)₂, гідроксид нікелю

1. Introduction

The modern world is facing the problem of depleting energy resources. The problem can be solved in two ways: employment of new energy sources or/and lowering of energy consumption by utilizing so-called "smart" technologies.

One promising division of "smart" technology is "smart" windows. These devices can dynamically change their optical characteristics – color, transparency, glossiness. In turn, this allows for significant cost savings on air conditioning and lighting and reducing loads on power grids at peak consumption times [1].

As of the present, active elements of smart windows have a number of issues. Insufficient transparency, constant current consumption in one of states and high cost of used active element types limit their application.

Unlike currently used systems, electrochemical solid-state systems have a number of advantages. High optical characteristics, power consumption only for state switch and potentially lower cost result in high chances for adoption.

Despite such chances, a few factors limit their application. For Ni(OH)₂ thin films, which are viewed as promising electrochemical electrochromic elements, have some disadvantages. Gradual degradation over a cycling period [2], insufficient adhesion to the substrate [3, 4], and lack of information regarding some operation aspects limit their application.

Nickel (II) hydroxide is anodic electrochromic material [5, 6]. It switches from transparent to dark-brown upon anodic polarization according to the following reaction (1):

$$Ni(OH)_2[transparent] \rightarrow NiOOH[dark\text{-}brown] + H^+ + \bar{e}. \quad (1)$$

Reaction (1) is reversed upon cathodic polarization, and colored NiOOH transforms back into transparent $Ni(OH)_2$.

2. Literature review and problem statement

The described reaction (1) occurs during polarization with external current, the parameters of which can be different. Supply of controlling current changes if it's used for state maintenance or switching, which depends on parameters of polarizing current: current density or potential (voltage for assembled device). As such, electrochemical electrochromic devices can operate in potentiostatic [7, 8], potentiodynamic [9, 10], galvanostatic [11] and galvanodynamic regimes. The latter regime is used rarely and primarily for special purposes. For real electrochemical systems, each regime has its advantages and disadvantages. Cycling in potentiostatic and potentiodynamic regimes can help avoiding undesired processes, such as oxygen evolution on nickel oxide electrode [12, 13]. In cases of $Ni/Ni(OH)_2$, side reaction can be limited with the use of the potentiostatic regime with limited maximum potential, or voltage for the assembled device [14, 15]. These regimes also prevent polarity switch of electrodes, which can be problematic when galvanostatic regimes are used. The disadvantage of potentiostatic regimes is a high initial current on device switching, which can cause overheating of some cell elements.

On the other hand, galvanostatic regimes are simpler in realization and allow for simple and easy control over electric current.

It is worth to note that the use of combined regimes is also possible. Such combined regimes can have advantages of both regimes.

Various modern papers serve as an example of different regimes used for cycling electrochemical devices. The paper [16] describes and discusses different regimes for accumulator charging and their influence on the resulting capacity of these electrochemical devices. The paper notes the importance of the regime for capacity testing and proposes the structure of the remote power grid based on modeling results.

The authors of the paper [17] propose a few variants of charge and discharge, which can extend the lifespan of batteries. They also note that operation characteristics are invariable of the proposed modification.

The current supply regime is of importance for electrochemical deposition of alloys. Thus, the authors of the paper [18] propose the impulse galvanostatic regime for deposition of Ni–Mo alloy. According to experimental results, they have found that a quality deposit requires the galvanostatic regime with current impulses with different duration and polarity. They also note that for chosen deposition regimes, reverse polarity impulses of 10–50 ms are important for deposition.

The authors of the other paper on electrochemical deposition of Co–Cu alloy [19] have employed the potentiostatic deposition regime. It is described that alloy composition, crystal structure and its magnetic properties are determined by the potential at which alloys are formed.

The paper on electrodeposition of Ni–Sn alloy [20] described the direct correlation between deposition regime and composition and morphology of deposits. The paper presents results of galvanostatic and potentiostatic regimes.

The analysis allows concluding that selection of appropriate cycling current parameters is of importance for electrochemical devices. Because no papers regarding the influence of cycling current on the operation of electrochromic materials were found, it was decided to conduct a series of experiments dedicated to this dependency.

3. The aim and objectives of the study

The aim of the work was to evaluate the influence of current supply regimes on electrochemical and electrochromic properties of $Ni(OH)_2$ films. Finding such dependencies would allow for simple selection of appropriate cycling regimes which would allow for better utilization and longevity of electrochromic devices.

To achieve the set aim, the following objectives must be completed:

– to prepare a series of identical electrochromic $Ni(OH)_2$ films using the cathodic template deposition method;

– to select a number of different cycling regimes and conduct their testing;

– to conduct a comparative analysis of electrochromic and electrochemical properties of films tested in different regimes.

4. Materials and methods used to study the influence of cycling regime on characteristics of electrochromic films

Reactants and materials used in the experiments

Analytical grade chemicals were used in all experiments. Glass electrodes coated with fluorine-doped SnO_2, then FTO glass (Zibo Lanjing Glass, China) were used as substrates for film deposition. Working electrode area 2×2 cm, sheet resistance 10 $\Omega/\square$.

All electrochromic films were prepared under conditions listed in Table 1.

Table 1

Conditions for film depositions using the cathodic template method

Electrolyte composition	Electrolyte temperature, °C	Cathodic current density, mA/cm^2	Deposition time, min
1 M $Ni(NO_3)_2$ 50 g/L PVA*	30	0.1	10

*Note: * – polyvinyl alcohol*

Flat nickel foil was used as anode [21].

Experimental regimes

For studying regimes, all film samples were prepared under standard conditions described above. As such, the cycling regime was the only experimental variable. A series of cycling regimes was proposed, all of which are listed in Table 2.

Studied regimes can be split into two categories. Simple, in which only one parameter – current or potential, was set, with separate stages being conducted over a set period of time. These are potentiodynamic and potentiostatic regimes (Table 2). The second type of regimes is labeled as complex. For these regimes, there was no set cycle time, as it was dependent on film behavior. For instance, for complex regime

No. 1, anodic current was switched off, only if the film potential was above 500 mV.

In order to determine current values for galvanostatic cycling, designated films were cycled in the standard potentiodynamic regime No. 1 and cathodic peak value was used as a starting point – notes to Table 2.

Table 2

Description of experimental regimes and sample labels[1]

Regime (Sample label)	Parameters
Potentiodynamic No. 1 (P1)	E_1=+201 mV, E_2=+751 mV; v=1 mV/s
Potentiodynamic No. 2 (P2)	E_1=+201 mV, E_2=+701 mV; v=1 mV/s
Potentiodynamic No. 3 (P3)	E_1=+201 mV, E_2=+801 mV; v=1 mV/s
Potentiodynamic No. 4 (P4)	E_1=+351 mV, E_2=+751 mV; v=1 mV/s
Potentiodynamic No. 5 (P5)	E_1=+ 451 mV, E_2=+751 mV; v=1 mV/s
Galvanostatic No. 1[2] (G1)	Step 1: I_a=+0.53 mA/s^2; τ_a=50 s; Step 2: I_k=−0.53 mA/s^2; τ_k=50 s
Galvanostatic No. 2[3] (G2)	Step 1: I_a=+0.88 mA/s^2; τ_a=25 s; Step 2: I_k=−+0.88 mA/s^2; τ_k=25 s
Complex No. 1[2](C1)	Step 1: I_a=+0.2 mA/s^2; τ_a=2.5 min; stop at E≥+701 mV; Step 2: I_k=−0.2 mA/s^2; τ_k=2.5 min; stop at E≤+201 mV;
Complex No. 2[3] (C2)	Step 1: I_a=+0.27 mA/s^2; τ_a=1.5 min; stop at E≥+701 mV; Step 2: I_k=−0.27 mA/s^2; τ_k=1.5 min; stop at E≤+201 mV; Step 3: E=−99 mV; τ=2.5 min

Notes: [1] – for galvanostatic regimes, the films were pre-cycled in the regime (P1) (201 – 751 mV, 1 mV/s), which was done to evaluate peak currents (maximum cathodic peak current on the fifth cycle) I_{CP}; [2] – $I_{(charge)}$=−I_{CP}; $I_{(discharge)}$=+I_{CP}; [3] – $I_{(charge)}$=−$2I_{CP}$; $I_{(discharge)}$=+$2I_{CP}$

It should be noted that for all graphs (Fig. 4–12, *a*), current values are re-calculated into current density (mA/s^2) based on the working electrode area of 4 cm^2.

Evaluation of electrochemical and optical characteristics of deposited films. Electrochemical cycling was conducted with simultaneous recording of the coloration-bleaching process using the custom-built cell, Fig. 1.

Ag/AgCl (KCl sat.) was used as a reference electrode, counter-electrode – nickel foil. Optical characteristics were recorded using ADC E-154 ("L-CARD", Russia) at the recording rate of 3 Hz, electrochemical parameters were set and recorded using the electronic potentiostat-galvanostat Ellins P-8 ("STF Volta", Russia).

Cycling regimes and potential windows are listed in Table 2. All experiments were conducted with 0.1 M KOH as an electrolyte.

At least five cycles were recorded, and for some (fast) regimes more than 20 to evaluate the influences of prolonged cycling. For cyclic voltamperometry curves (CVA), peak position, value and shape were analyzed, along with any curve differences on subsequent cycles.

Coloration-bleaching curves were analyzed for absolute coloration degree (D_n) –transparency difference between bleached and colored states on each cycle (n) and its aver-

aged value (D_a) according to Fig. 2. Coloration-bleaching curves were also used to derive absolute irreversibility (I_n) on each cycle (n) and its averaged value (I_a) – Fig. 3, equation (3). The shapes of the curves were also analyzed.
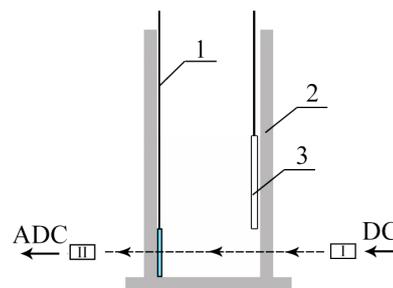

Fig. 1. Cell with the electrode for electrochemical and optical tests: 1 — working electrode with the deposited film; 2 — cell farm from transparent plastic; 3 — counter-electrode; I — source of white light (5,500 K); II — photoresistor. DC — source of stabilized constant voltage; ADC — analog-to-digital converter
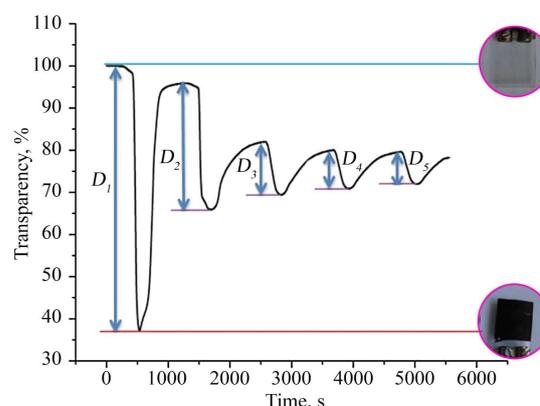

Fig. 2. Calculation of absolute coloration degree from bleaching-coloration curves

$$D_a = \sum_1^n \frac{D_n}{n}. \qquad (2)$$
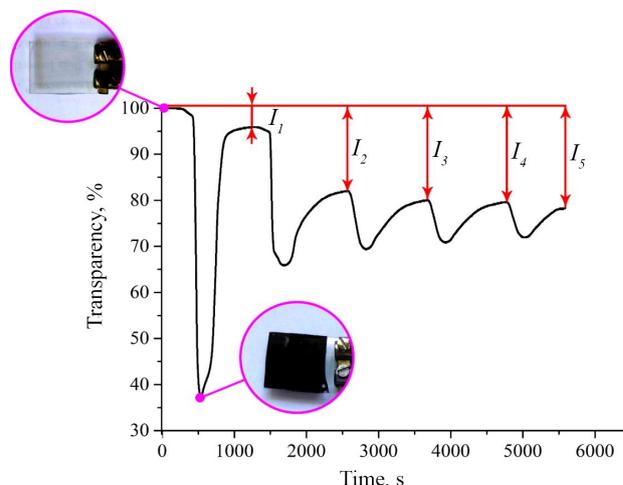

Fig. 3. Calculation of irreversibility from bleaching-coloration curves

$$I_a = \sum_1^n \frac{I_n}{n}. \qquad (3)$$

In addition, film uniformity and color were also evaluated after cycling.

5. Analysis and comparison of electrochemical and optical characteristics of samples tested in different regimes

In order to evaluate specific currents, films were cycled in standard potentiodynamic regime No. 1 and cathodic peak current was chosen as the starting point for regime testing – note to Table 2.

Potentiodynamic regimes P1, P2, P3, P4, P5

Results for cycling regime (P1), also referred to as "standard regime", are shown in Fig. 4. This regime is referred to as standard because it was used for film testing in our previous works on nickel hydroxide-based electrochromic materials [3, 4, 10, 12, 21]. It was also used for preliminary cycling before galvanostatic and complex regimes. Analysis of the cyclic voltamperometry (CVA) curve, shown in Fig. 4, allows drawing a few important conclusions. First, the characteristics of the film gradually decrease with cycling – peak currents decrease and shift slightly with each cycle (the shifts are indicated by red arrows). Second, current values of reduction and oxidation peaks are close, with the exception of the first cycle, which indicates good capacitive efficiency. It worth to note that peak height is a parameter which can be used for semi-quantitative evaluation of the peak area. In turn, the peak area corresponds to the capacity used for the oxidation/reduction process.

Fig. 4, *b* shows photographs of the colored electrochromic film after potentiodynamic regime P1. The film has a uniform dark color across the entire working area, indicating the high quality of the sample. It is interesting that the back side of the electrode has violet gloss upon reflection of direct light.

The coloration-bleaching curve shown in Fig. 4 *c* allows concluding that under this regime, the film shows a rather high coloration degree and negligible irreversibility during bleaching. In addition, the shape of the coloration-bleaching curve is close to rectangular. For electrochromic materials, such shape is close to ideal, i. e. rectangular.

For potentiodynamic regime P2, the potential window was shortened in comparison with standard – E [+201; +751 mV]. The CVA curve for this regime showed some worsening of electrochemical characteristics – Fig. 5, *a*. The cathodic peak current was significantly lower than anodic, and peaks shifting is similar to CVA of the previous regime. It is interesting that after the left peak, there is a plateau with the height of about 30 % of the cathodic peak. It obvious that narrowing of potential borders from the left side (in more negative region) results in the incomplete reduction of the film.

The photographs shown in Fig. 5, b reveal that the film cycled in this regime has a uniform dark color, similar to that in the previous experiment.

The coloration - bleaching curve of this regime showed characteristics similar to those of the previous regime – Fig. 5, *c*. Reversibility of the coloration-bleaching process is high, while coloration degree is somewhat lower.

For potentiodynamic regime P3, the cycling potential window was extended, compared to standard (750 mV) and was E [+201; +801 mV]. Because of such change, an elevation appeared at about 750 mV, which is caused by oxygen evolution (Fig. 6, *a*). The shape of the CVA curve and its values are similar to those of potentiodynamic regime P1.
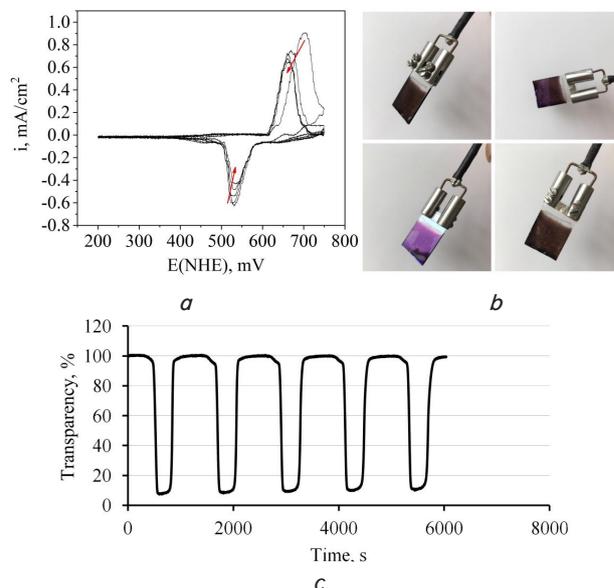

Fig. 4. Results for regime P1: *a* — CVA curve of the electrode recorded in the potentiodynamic regime; *b* — photograph of the electrode in the colored state after testing; *c* — coloration-bleaching curve

Photographs of the colored film after potentiodynamic cycling P3 are shown in Fig. 6, *b*. It should be noted that the film on the electrode surface has a uniform dark color, similar to previous regimes. However, the electrode shows the presence of transparent areas. This is undoubtedly caused by the side reaction of oxygen evolution, which causes the formation of oxygen bubbles that tear the film off from the substrate.

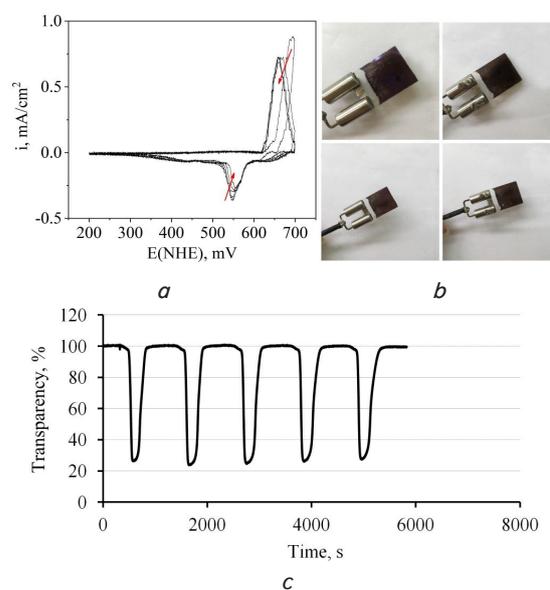As with CVA, the coloration-bleaching curve is similar to that of the standard regime (potentiodynamic regime P1).

Fig. 5. Results for regime P2: *a* — CVA curve of the electrode recorded in the potentiodynamic regime; *b* — photograph of the electrode in the colored state after testing; *c* — coloration-bleaching curve

For potentiodynamic regime P4, the potential window was reduced to E [+351; +751 mV]. Such reduction led to a significant decrease of electrochemical characteristics (dif-

ferent heights of anodic and cathodic peaks) and optical characteristics (lower coloration degree, rounding of the coloration-bleaching curve) – Fig. 7, *a, c.* Photographs of the electrode after cycling revealed imperfections in film coloration: a large number of transparent spots, non-uniform color – Fig. 7, *b.*
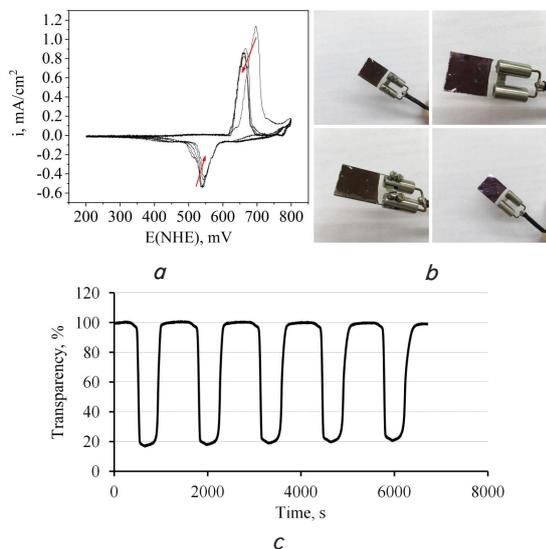

a

b

c

Fig. 6. Results for regime P3: *a* — CVA curve of the electrode recorded in the potentiodynamic regime; *b* — photograph of the electrode in the colored state after testing; *c* — coloration-bleaching curve

Further narrowing of the potential window to E [+451; +751 mV] resulted in a decrease of all characteristics: optical, electrochemical and qualitative. The peaks of the CVA curve had different heights, the shape of which (along with the overall shape of the curve) changed over time. Coloration-bleaching curve showed significant irreversibility during bleaching (Fig. 8, *a, c*). Photographs of colored films after cycling reveal large areas without film coloration and non-uniform color of the film – Fig. 8, *b.*
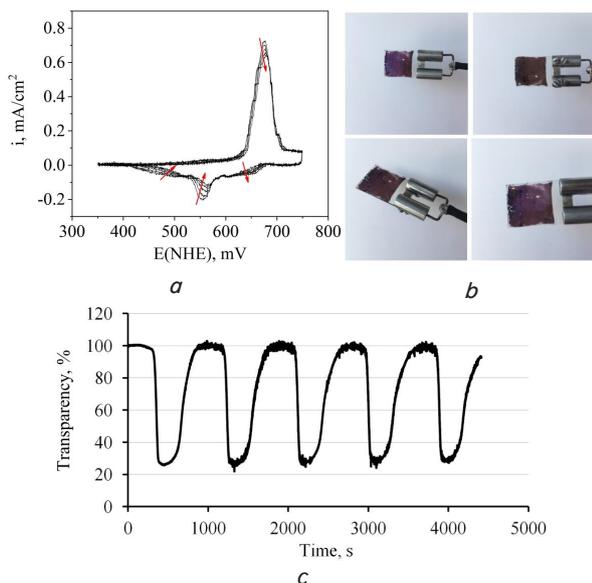

a

b

c

Fig. 7. Results for regime P4: *a* — CVA curve of the electrode recorded in the potentiodynamic regime; *b* — photograph of the electrode in the colored state after testing; *c* — coloration-bleaching curve
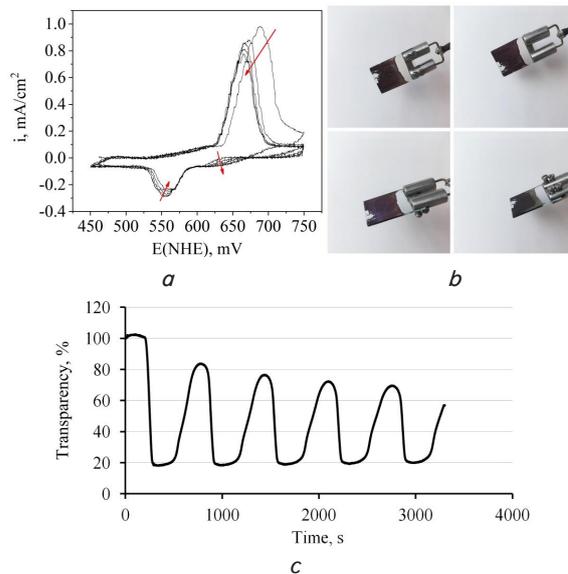

a

b

c

Fig. 8. Results for regime P5: *a* — CVA curve of the electrode recorded in the potentiodynamic regime; *b* — photograph of the electrode in the colored state after testing; *c* — coloration-bleaching curve

Galvanostatic regimes G1, G2

The next stage in the study on the influence of the cycling regime on optical and electrochemical characteristics are regimes with a constant current. Prior to testing, each film was cycled in the standard regime (P1). Next, the cathodic peak current at the fifth cycle was used for polarization in the galvanostatic regime (I_{CP}).

Fig. 9 shows results for the film cycled in the galvanostatic regime G1. Fig. 9, *a* shows potential over time and current over time curves. Analysis of these curves revealed that the electrode potential immediately rises to about 670 mV and remains constant over the entire period of anodic polarization. The potential curve during the cathodic period shows two plateaus, which can correspond to different phases. It is possible that the synthesis method resulted not in the formation of pure α-Ni(OH)$_2$ but into a mixture of α and β phases [22–25]. The latter would result in two plateaus. Coloration-bleaching curves of 25 cycles revealed stable optical characteristics but lower coloration degree than that of the standard regime (potentiodynamic regime P1) – Fig. 4.

Photographs of the films subjected to cycling in galvanostatic regime G1 are shown in Fig. 9, *b.* Uniform coloration and absence of transparent spots on the electrode indicate that this regime is suitable for bleaching-coloration cycling and does not result in film peeling.

Galvanostatic regime G2 differs from the previous one in that used current densities are two times of the cathodic peak current ($2*I_{CP}$). Results for this regime are shown in Fig. 10. Dependencies of the electrode potential and current density on time, shown in Fig. 10, *a*, demonstrate behavior similar to the previous regime – potential spike (~+700 mV) on anodic polarization and two plateaus on cathodic polarization. Coloration-bleaching curve for this regime also showed a lower coloration degree in comparison with the standard regime (P1). However, the coloration degree is lower than that of the previous galvanostatic regime. It is evident that high cycling current density has a negative effect on coloration degree.

Photographs of the electrode after cycling in this regime (G2) are shown in Fig. 10, *b*. It should be noted that electrochromic films have no major defects, with deep and uniform coloration.
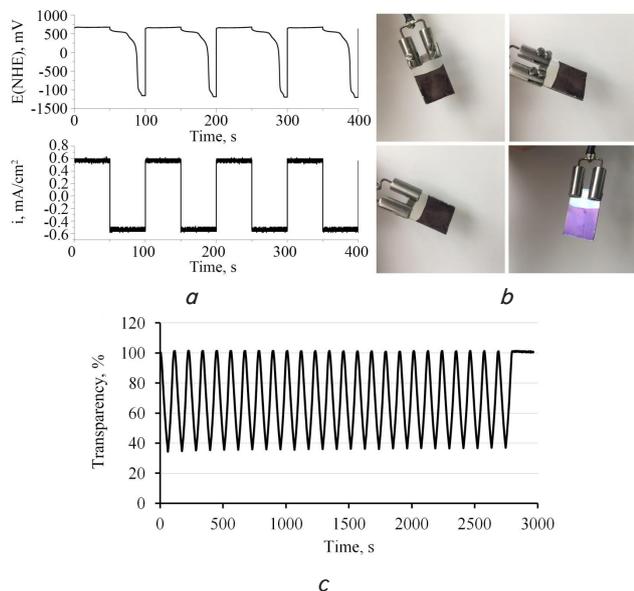

c

Fig. 9. Results for regime G1:
a — electrode curve recorded in the galvanostatic regime (potential and current dependencies on time, 1 — 4 cycle);
b — photograph of the colored electrode after cycling;
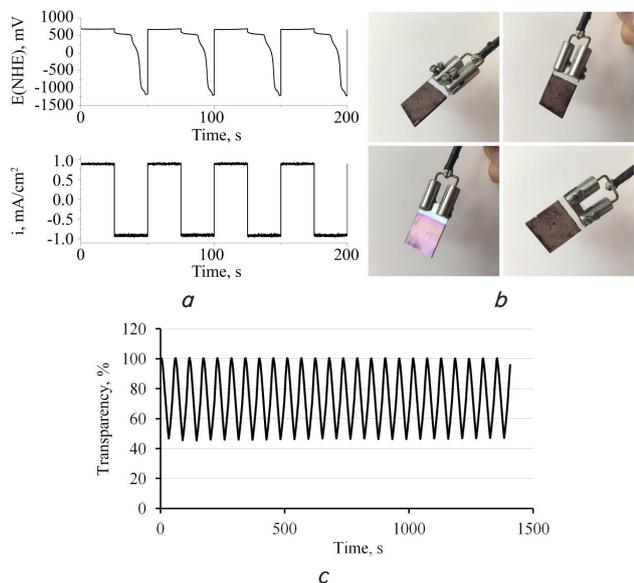*c* — coloration-bleaching curve

c

Fig. 10. Results for regime G2:
a — electrode curve recorded in the galvanostatic regime (potential and current dependencies on time, 1 — 4 cycle);
b — photograph of the colored electrode after cycling;
c — coloration-bleaching curve

Complex regimes C1, C2

The third stage of research is cycling of electrochromic films in complex regimes.

For complex regime C1, galvanostatic anodic and cathode polarizations periods were used. Polarization was stopped after achieving certain potential values. The anodic period lasted until the electrode potential reached +701 mV.

For the cathodic period, the negative current was kept constant until the potential reached +201 mV (Fig. 11, *a*). As such, the duration of cathodic and anodic periods was different. Complex regime No. 1 did not yield great results as coloration depth was low and irreversibility on bleaching was higher than zero – Fig. 11. Photograph of the film after cycling in complex regime C1 is shown in Fig. 11, *b*.

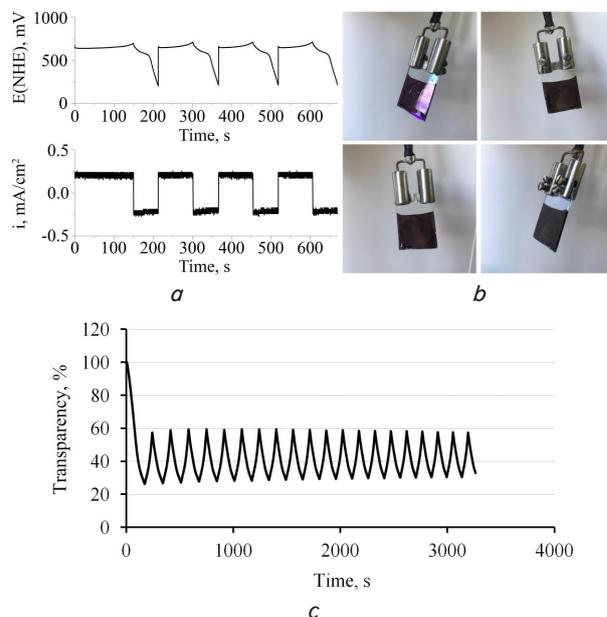Based on these results, it was decided to change the complex regime.

c

Fig. 11. Results for complex regime C1:
a — electrode curve recorded in the complex regime (potential and current dependencies on time, 1 — 4 cycle);
b — photograph of the colored electrode after cycling;
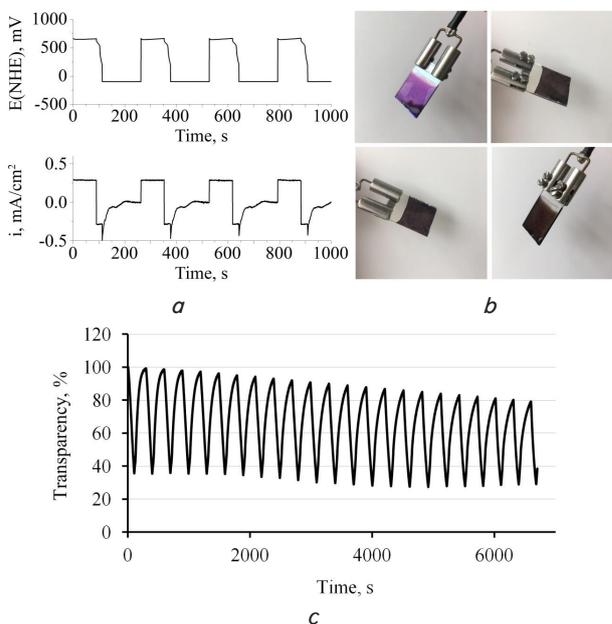*c* — coloration-bleaching curve

c

Fig. 12. Results for complex regime C2:
a — electrode curve recorded in the complex regime (potential and current dependencies on time, 1 — 4 cycle);
b — photograph of the colored electrode after cycling;
c — coloration-bleaching curve

Complex regime C2 is a modification of the previous regime. An additional stage was added, which allowed for the complete bleaching of the film. An additional step was added after the cathodic period. For this step, the film was kept at the potential of –99 mV for 2.5 minutes (Fig. 12). This resulted in higher characteristics in comparison to regime C1: higher coloration degree and lower irreversibility on bleaching (Fig. 12, b). However, the regime is not ideal – some degradation of electrochromic properties was observed. Photographs of the colored film after cycling in regime C2 are shown in Fig. 12, b.

6. Discussion of the result for electrochromic films cycled in different regimes

In general, it can be said that potentiodynamic regimes with slow scan rate can be used for evaluating the maximum coloration degree. However, such regimes do not allow for fast color switching. Narrowing of potential borders from either side results in lowered parameters of electrochromic films. On the other hand, widening of potential windows to the anodic region causes film peeling off due to oxygen evolution. Thus, it can be concluded that cycling of electrochromic nickel hydroxide films past +750 mV is not viable, because of film peeling.

Galvanostatic regimes are simpler to implement, however, polarization with current close to the peak current of CVA leads to a lower value of absolute coloration degree, in comparison with the standard regime. Increasing current over I_{CP} results in the decrease of coloration degree.

Testing in complex regimes yielded ambiguous results. It should be noted that complex regimes chosen in this study do not meet qualitative criteria for electrochromic devices. However, an even larger number of regime variants needs to be studied, which is the subject for future studies.

For a summary, all results were compiled into histograms which include averaged absolute coloration degree (D_a) and averaged absolute irreversibility on bleaching (I_a) – Fig. 13. For a better understanding of time required for coloration and bleaching, coloration and bleaching times were plotted onto the histogram – Fig. 13. A few important conclusions can be derived from these histograms. Despite the use of different regimes, the standard regime (P1) shows the highest averaged absolute coloration degree. On the other hand, averaged irreversibility on bleaching is lower in potentiodynamic and galvanostatic regimes. Chosen complex regimes loose in averaged coloration degree and show higher averaged irreversibility on bleaching. Nevertheless, it is possible that further modification of complex regimes can lead to optimal parameters for film cycling.

When evaluating regimes, it is important to consider not only qualitative characteristics from each regime, but also consider the duration of the coloration/bleaching process. From the perspective of minim duration and maximum qualitative characteristics, galvanostatic regimes are in favor – G1 and G2 (Fig. 14).

In conclusion, it is worth to note that while chosen regimes do not cover all possible variants, the conducted experiments allow for qualitative evaluation of differences of electrochromic and electrochemical characteristics between cycling regimes and their parameters. This would allow for future optimization in cycling parameters for electrochromic devices.
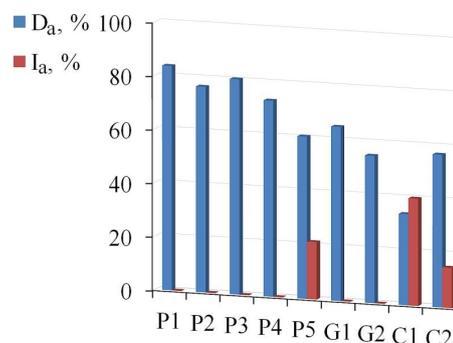

Fig. 13. Histogram with resulting averaged coloration degree (D_a) and absolute irreversibility on bleaching (I_a) for each regime
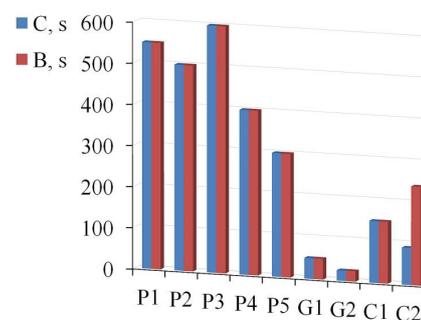

Fig. 14. Histogram with resulting times for coloration (C) and bleaching (B) for each regime

7. Conclusions

1. For the demonstration of electrochromic and electrochemical characteristics, the most suitable is potentiodynamic regime P1: E [+201; +751 mV] with the scan rate of 1 mV/s.

2. The optimal regimes for electrochromic and electrochemical characteristics and time required per cycle are:

a) galvanostatic regime G1:

$I_a=+I_{CP}$, $\tau_A=50$ s; $I_C=-I_{CP}$, $\tau_C=50$ s;

b) galvanostatic regime G2:

$I_a=+2I_{CP}$, $\tau_A=25$ s; $I_C=-2\cdot I_{CP}$, $\tau_C=25$ s.

3. For chosen potentiodynamic regimes, narrowing of cycling potential window led to a significant decrease of optical and electrochemical characteristics of the films. Peak currents decreased by 2 times, absolute coloration by 23 % and averaged irreversibility on bleaching increased to 21 %. Increasing current for galvanostatic regimes also resulted in a decrease of optical characteristics. Doubling the current from initial I_{CP} resulted in a decrease of coloration degree by 10 %.

References

1. Smart Windows: Energy Efficiency with a View. URL: https://www.nrel.gov/news/features/2010/1555.html
2. Electrochemical Rejuvenation of Anodically Coloring Electrochromic Nickel Oxide Thin Films / Qu H.-Y., Primetzhofer D., Arvizu M. A., Qiu Z., Cindemir U., Granqvist C. G., Niklasson G. A. // ACS Applied Materials & Interfaces. 2017. Vol. 9, Issue 49. P. 42420–42424. doi: https://doi.org/10.1021/acsami.7b13815

3. Advanced electrochromic Ni(OH)$_2$/PVA films formed by electrochemical template synthesis / Kotok V. A., Kovalenko V. L., Kovalenko P. V., Solovov V. A., Deabate S., Mehdi A. et. al. // ARPN Journal of Engineering and Applied Sciences. 2017. Vol. 12, Issue 13. P. 3962–3977.

4. Effect of deposition time on properties of electrochromic nickel hydroxide films prepared by cathodic template synthesis / Kotok V. A., Kovalenko V. L., Solovov V. A., Kovalenko P. V., Ananchenko B. A. // ARPN Journal of Engineering and Applied Sciences. 2018. Vol. 13, Issue 9. P. 3076–3086.

5. Electrochemical and Electrochromic Properties of Ni Oxide Thin Films Prepared by a Sol–Gel Method / Park J.-Y., Ahn K.-S., Nah Y.-C., Shim H.-S., Sung Y.-E. // Journal of Sol-Gel Science and Technology. 2004. Vol. 31, Issue 1-3. P. 323–328. doi: https://doi.org/10.1023/b:jsst.0000048011.77244.5e

6. Al-Kahlout A., Pawlicka A., Aegerter M. Brown coloring electrochromic devices based on NiO–TiO$_2$ layers // Solar Energy Materials and Solar Cells. 2006. Vol. 90, Issue 20. P. 3583–3601. doi: https://doi.org/10.1016/j.solmat.2006.06.053

7. Substrate-Friendly Growth of Large-Sized Ni(OH)$_2$ Nanosheets for Flexible Electrochromic Films / Zhu L., Ong W. L., Lu X., Zeng K., Fan H. J., Ho G. W. // Small. 2017. Vol. 13, Issue 23. P. 1700084. doi: https://doi.org/10.1002/smll.201700084

8. Electrochromo-supercapacitor based on direct growth of NiO nanoparticles / Cai G., Wang X., Cui M., Darmawan P., Wang J., Eh A. L.-S., Lee P. S. // Nano Energy. 2015. Vol. 12. P. 258–267. doi: https://doi.org/10.1016/j.nanoen.2014.12.031

9. The improving electrochromic performance of nickel oxide film using aqueous N,N-dimethylaminoethanol solution / Park S. H., Lim J. W., Yoo S. J., Cha I. Y., Sung Y.-E. // Solar Energy Materials and Solar Cells. 2012. Vol. 99. P. 31–37. doi: https://doi.org/10.1016/j.solmat.2011.06.023

10. Kotok V., Kovalenko V. The electrochemical cathodic template synthesis of nickel hydroxide thin films for electrochromic devices: role of temperature // Eastern-European Journal of Enterprise Technologies. 2017. Vol. 2, Issue 11 (86). P. 28–34. doi: https://doi.org/10.15587/1729-4061.2017.97371

11. Nitrogen-doped nickel oxide thin films for enhanced electrochromic applications / Lin F., Gillaspie D. T., Dillon A. C., Richards R. M., Engtrakul C. // Thin Solid Films. 2013. Vol. 527. P. 26–30. doi: https://doi.org/10.1016/j.tsf.2012.12.031

12. Kotok V., Kovalenko V., Malyshev V. Comparison of oxygen evolution parameters on different types of nickel hydroxide // Eastern-European Journal of Enterprise Technologies. 2017. Vol. 5, Issue 12 (89). P. 12–19. doi: https://doi.org/10.15587/1729-4061.2017.109770

13. Snook G. A., Duffy N. W., Pandolfo A. G. Evaluation of the effects of oxygen evolution on the capacity and cycle life of nickel hydroxide electrode materials // Journal of Power Sources. 2007. Vol. 168, Issue 2. P. 513–521. doi: https://doi.org/10.1016/j.jpowsour.2007.02.060

14. All-solid-state electrochromic device composed of WO$_3$ and Ni(OH)$_2$ with a Ta$_2$O$_5$ protective layer / Ahn K.-S., Nah Y.-C., Sung Y.-E., Cho K.-Y., Shin S.-S., Park J.-K. // Applied Physics Letters. 2002. Vol. 81, Issue 21. P. 3930–3932. doi: https://doi.org/10.1063/1.1522478

15. Polymer-Laminated Electrochromic Devices Composed of WO$_3$ and Ni(OH)$_2$ on Glass and PET Substrates / Nah Y.-C., Ahn K.-S., Cho K.-Y., Park J.-Y., Shim H.-S., Lee Y. M. et. al. // Journal of The Electrochemical Society. 2005. Vol. 152, Issue 12. P. H201–H204. doi: https://doi.org/10.1149/1.2073088

16. Comparative Analysis of Battery Behavior with Different Modes of Discharge for Optimal Capacity Sizing and BMS Operation / Abbas M., Kim E., Kim S., Kim Y. // Energies. 2016. Vol. 9, Issue 10. P. 812. doi: https://doi.org/10.3390/en9100812

17. Optimization of Charge/Discharge Rates of a Battery Using a Two-Stage Rate-Limit Control / Kollimalla S. K., Ukil A., Gooi H. B., Manandhar U., Tummuru N. R. // IEEE Transactions on Sustainable Energy. 2017. Vol. 8, Issue 2. P. 516–529. doi: https://doi.org/10.1109/tste.2016.2608968

18. Study of Ni-Mo electrodeposition in direct and pulse-reverse current / Stryuchkova Y. M., Rybin N. B., Suvorov D. V., Gololobov G. P., Tolstoguzov A. B., Tarabrin D. Y. et. al. // Journal of Physics: Conference Series. 2017. Vol. 857. P. 012046. doi: https://doi.org/10.1088/1742-6596/857/1/012046

19. Influence of the electrodeposition potential on the Co-Cu alloys thin films properties / Mentar L., Khelladi M. R., Beniaiche A., Azizi A. // International Journal of Nanoscience. 2013. Vol. 12, Issue 1. P. 1250038. doi: https://doi.org/10.1142/s0219581x1250038x

20. Rudnik E., Włoch G., Czernecka A. The influence of potential-current conditions on the electrodeposition of Ni-Sn alloys from acidic chloride-sulphate solution // Archives of Metallurgy and Materials. 2014. Vol. 59, Issue 1. P. 195–198. doi: https://doi.org/10.2478/amm-2014-0031

21. Soft Electrochemical Etching of FTO-Coated Glass for Use in Ni(OH)$_2$-Based Electrochromic Devices / Kotok V. A., Malyshev V. V., Solovov V. A., Kovalenko V. L. // ECS Journal of Solid State Science and Technology. 2017. Vol. 6, Issue 12. P. P772–P777. doi: https://doi.org/10.1149/2.0071712jss

22. Nickel hydroxides and related materials: a review of their structures, synthesis and properties / Hall D. S., Lockwood D. J., Bock C., MacDougall B. R. // Proceedings of the Royal Society A: Mathematical, Physical and Engineering Sciences. 2014. Vol. 471, Issue 2147. P. 20140792–20140792. doi: https://doi.org/10.1098/rspa.2014.0792

23. Srinivasan V., Weidner J. W., White R. E. Mathematical models of the nickel hydroxide active material // Journal of Solid State Electrochemistry. 2000. Vol. 4, Issue 7. P. 367–382. doi: https://doi.org/10.1007/s100080000107

24. Delahaye-Vidal A. Structural and textural investigations of the nickel hydroxide electrode // Solid State Ionics. 1996. Vol. 84, Issue 3-4. P. 239–248. doi: https://doi.org/10.1016/0167-2738(96)00030-6

25. Kovalenko V., Kotok V. Comparative investigation of electrochemically synthesized (α+β) layered nickel hydroxide with mixture of α-Ni(OH)$_2$ and β-Ni(OH)$_2$ // Eastern-European Journal of Enterprise Technologies. 2018. Vol. 2, Issue 6 (92). P. 16–22. doi: https://doi.org/10.15587/1729-4061.2018.125886